Marine Geology 440 (2021) 106548

Contents lists available at ScienceDirect

Marine Geology

journal homepage: www.elsevier.com/locate/margo

Research Article

How volcanically active is an abyssal plain? Evidence for recent volcanism on 20 Ma Nazca Plate seafloor

C.W. Devey [a,*], J. Greinert [b], A. Boetius [c], N. Augustin [a], I. Yeo [a,1]

[a] Seafloor Volcanism, Geomar Helmholtz Centre for Ocean Research Kiel, Wischhofstr. 1-3, 24148 Kiel, Germany
[b] DeepSea Monitoring, Geomar Helmholtz Centre for Ocean Research Kiel, Wischhofstr. 1-3, 24148 Kiel, Germany
[c] Alfred-Wegener-Institut, Helmholtz Centre for Polar and Marine Research, Am Handelshafen 12, 27570 Bremerhaven, Germany

ARTICLE INFO

Editor: Michele Rebesco

Keywords:
Volcanism
Intraplate
Peru Basin
Non-hotspot

ABSTRACT

The abyssal plains are generally assumed to be geologically inactive parts of the ocean plate interiors where processes (such as pelagic sedimentation or manganese crust and nodule formation) occur at very slow rates. In terms of intraplate volcanic activity, almost all is assumed to occur at hotspots, leading to little exploration in other intraplate regions. The Peru Basin is an abyssal plain known to host Mn-nodule fields. We present remotely-operated underwater vehicle (ROV) investigations of a small seamount adjacent to such a Mn-nodule field on 20Ma Nazca Plate crust, showing that it appears to have been recently volcanically and hydrothermally active. The seamount lies 1600km east of the nearest spreading axis (East Pacific Rise) and 600km from both the Galapagos Plateau (to the north) and the subduction zone off Peru (to the east), making off-axis, hotspot or petit-spot processes unlikely as a cause of the volcanism. The shallow mantle below the Nazca (and conjugate Pacific) Plate shows globally anomalous low seismic shear-wave velocities, perhaps reflecting higher-than-normal amounts of melt in the mantle below this region which may provide a source for the magmas. Our own regional mapping work and literature sources highlight several similar sites of probable young volcanism elsewhere in the Peru Basin which may also be related to this anomaly. The Nazca abyssal plain may be much more geologically active than previously thought. If so, this could have wider implications for, among other things, chemosynthetic ecosystem connectivity.

1. Introduction

Volcanism in the ocean basins is traditionally assumed to occur almost exclusively at the plate margins (mid-ocean ridges, subduction zones, possibly also transform boundaries) and areas of intraplate hotspot activity related to thermo-chemical plumes in the mantle (Morgan, 1971). Some exceptions to this general scheme are known, all producing large volcanic features visible on satellite altimetry maps (Smith and Sandwell, 1997): In the Pacific, elongated intraplate volcanic ridges have been discovered and proposed to be caused by shear-driven upwelling in the asthenosphere (e.g., Pukapuka, Sojourn and Hotu-Matua Ridges, South Pacific: Ballmer et al., 2013; Holmes et al., 2007) or to breaking of the Farallon plate (Alvarado and Samiento Ridges: Lonsdale, 2005; see also Fig. 1); in the Atlantic, isolated volcanoes have been related to intraplate stress fields leading to lithospheric extensional fractures (Haase and Devey, 1994) or to small melting anomalies in the vicinity of plumes (Long et al., 2020). Recent ship-based exploration has revealed small volcanoes not visible on satellite maps on the Pacific plate off Japan (Harigane et al., 2011; Hirano et al., 2001) and on the Nazca plate off Chile (Hirano et al., 2013). These petit spots are thought to be related to plate flexure prior to subduction (Hirano et al., 2006). Whether small-volume volcanism is also a feature of the ocean floor away from subduction zone flexure was, until now, largely unexplored. The aim of this paper is to present first results from volcanic exploration in the Peru Basin, an intraplate abyssal area far from plate boundaries or hotspots. The area has previously been the subject of Mn-nodule-mining environmental impact studies (the DISCOL project: Borowski and Thiel, 1998; Thiel et al., 2001). We find clear evidence for relatively recent magmatic activity in the region.

* Corresponding author.
E-mail address: cdevey@geomar.de (C.W. Devey).
[1] Present address: National Oceanography Centre, Southampton, UK.

https://doi.org/10.1016/j.margeo.2021.106548
Received 4 June 2019; Received in revised form 18 June 2021; Accepted 26 June 2021
Available online 29 June 2021

2. Geological setting

The study region, which we will henceforth refer to as "the DISCOL area" lies in the Peru Basin on the Nazca plate (Fig. 1). Regional inferred bathymetry from satellite altimetry and occasional ship tracks, combined in the GEBCO grid (www.gebco.net), is presented on Fig. 1. This figure also shows new multibeam mapping data collected by us in the course of the work described here (data sources are given in the figure caption), these data already are (https://doi.pangaea.de/10.1594/PANGAEA.854125) or will be made available at the Pangaea World Data Centre www.pangaea.de prior to publication. Fig. 1 shows no seamount chains or large tectonic features within several hundred kilometers of the DISCOL area, although some isolated seamounts are seen which will be discussed later. The large Alvarado and Sarmiento ridges are thought to represent fissures related to the initial stages of break-up of the Farallon plate (Lonsdale, 2005). This break-up eventually created the Cocos and Nazca plates by rupture along the Grijalva Scarp around 23 Ma (Castillo and Lonsdale, 2004; Lonsdale, 2005). A compilation of magnetic anomalies (Lonsdale, 2005) suggests that the seafloor in the DISCOL region was created at the East Pacific Rise around 20 Ma ago (magnetic anomaly 6A, Lonsdale, 2005). The DISCOL area is ca. 600 km south of the margin of the Galapagos Plateau, over 600 km west of the outer margin of the Peruvian subduction zone and 1.600 km east of the East Pacific Rise. The average depth of the region (between 4200 and 4100 m) is in accordance with the 4150 m predicted for a 20 Ma old plate by subsidence models (Korenaga and Korenaga, 2008). An overview map of the bathymetry of the DISCOL area is shown in Fig. 2.

As part of a 2015 environmental survey (Drazen et al., 2019; Gausepohl et al., 2020; Simon-Lledo et al., 2019), an autonomous biogeochemical station ("lander") was deployed outside the DISCOL disturbance area to study background values of ocean currents and other physical properties (see Boetius, 2015). Following deployment, the lander failed to respond to releaser signals and so in a (finally unsuccessful) effort to recover it, the last remotely operated vehicle (ROV) dive of cruise SO-242/2 (station 235ROV) made a detailed visual search of the seafloor at the lander deployment area of the seamount summit. No samples were collected during this search.

The area of the ROV survey lies on the small seamount to the north-northeast of the DISCOL disturbance patch (Fig. 2). The new bathymetric data show this seamount to have an irregular shape, with several small circular cones visible on its flanks. The seamount itself and its flanking cones show the steepest slopes in the area (up to 30°) as well as higher rugosity than the surrounding seafloor (rugosities of up to 1.14 are evident on the seamount, where rugosity is defined as the ratio of the area of a 3 × 3 grid square in the digital terrain model (DTM) to the area of a horizontal plane covering the same grid points. The DTM used for this calculation has 50x50m cells). The seamount rises from a broader plateau at around 4150 m to the shallowest summit at 3850 m. This peak depth is much shallower than the carbonate compensation depth in the South Pacific and close to the lysocline there (Pälike et al., 2012; Rea and Leinen, 1985). Data from ODP drilling (Lyle, 1992) show surface sediments in this region to have carbonate accumulation rates up to ca. 700 mg cm^{-2} $k.a.^{-1}$ and indicate a carbonate/opal ratio in the sediments >1. Sediment analyses from gravity cores taken during the cruise on which the ROV dive took place show three distinct carbonate enriched layer, one at the sediment surface (up to15 wt% Ca), one near the sediment surface (~20 wt% Ca, at 1–5 mbsf) and a third one in about 8–10 m depth with ~20 wt% Ca (Paul et al., 2019).

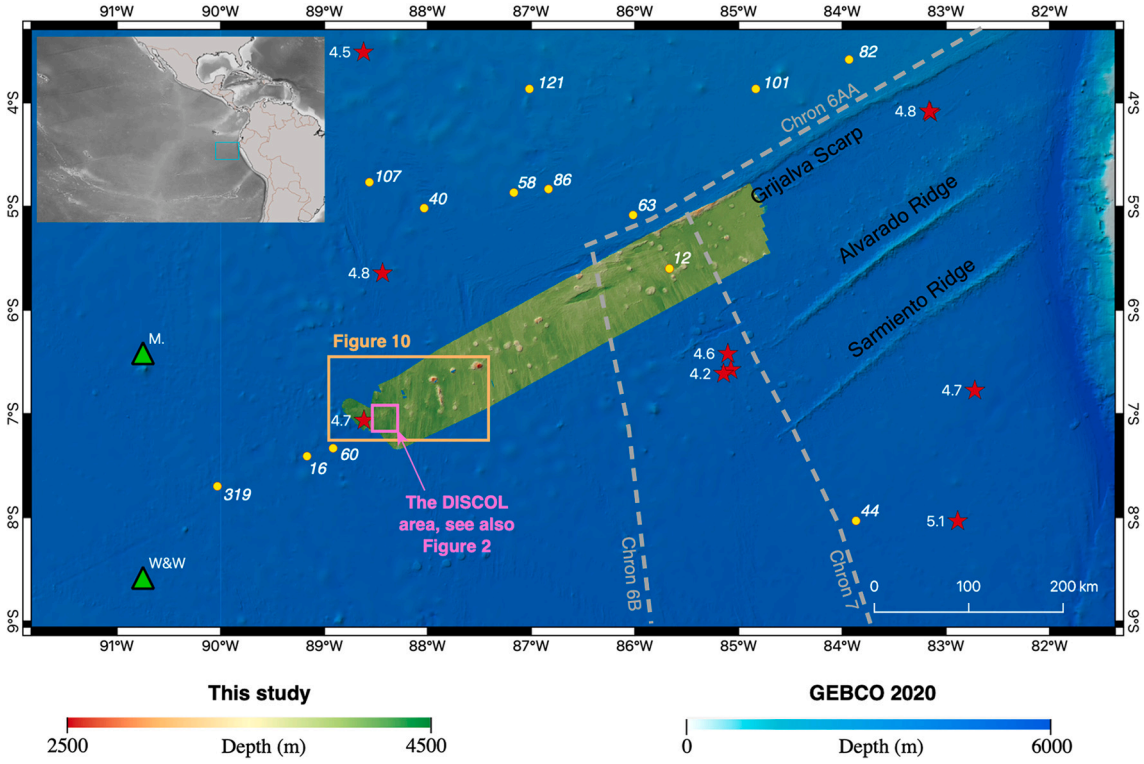

Fig. 1. Main figure: The location of the DISCOL area within the Pacific ocean. Major topographic features on the Nazca plate mapped (but not sampled) by Lonsdale (2005) are labelled as are selected isochrons (grey dashed lines) on crust formed at the Pacific-Farallon (NW-SE trending) and Cocos-Nazca (NE-SW trending) plate boundaries. Yellow circles show the location of heatflow measurements (values in mW/m^2). Red stars show locations of earthquakes recorded in the IRIS catalogue since 1970 (from iris.edu, last updated 17 June 2021). Green triangles show the locations of seamounts studied by Marchig et al. (1999) labelled "M." and Wiedicke and Weber (1996) labelled "W&W". Note the different and mutually exclusive colour scales for the regional GEBCO map (blues) and the area mapped during cruises SO-242/1 and SO-242/2 reported here (green/red). Raw bathymetric data from these cruises are available at https://doi.pangaea.de and https://doi.org/10.1594/PANGAEA.854125). *Inset top left:* Grey-scale bathymetry of the NE equatorial Pacific showing location of the main figure (blue box). (For interpretation of the references to colour in this figure legend, the reader is referred to the web version of this article.)

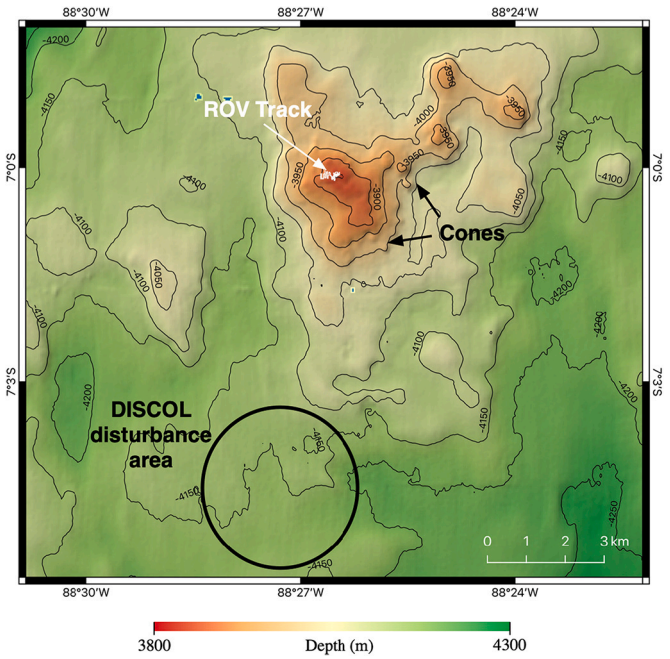

Fig. 2. The bathymetry of the study area derived from the 2015 multibeam data collected during cruise SO-242/2. The area disturbed during the original DISCOL project is marked, as are cones visible on the seamount flank and the track (in white) of the ROV dive reported here (see also Figs. 3 and 9). The bathymetric grid from which this figure was produced is from Gausepohl et al. (2020) and can be downloaded at https://doi.org/10.1594/PANGAEA.905579".

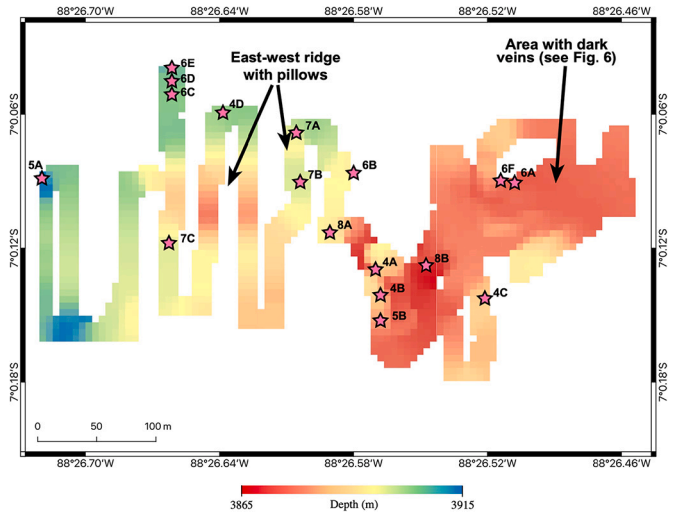

Fig. 3. Gridded ROV bathymetry (obtained from ROV altitude plus depth). Note that due to navigational inaccuracies inherent in the ROV work, only the general structure of the seafloor is available from this map. Labelled areas refer to features described under "4.2 Geological Observations". Stars show the locations of individual seafloor photographs presented in Figs. 4-8, labelled with figure number and sub-panel letter.

3. Methods

Video investigations were performed with the ROV Kiel6000 run by GEOMAR. The vehicle has a maximum operating depth of 6000 m and is equipped with both standard-definition (SD or 480p) and high-definition (HD or 1080p) video cameras mounted on pan-tilt heads. The HD video provided most of the images presented in this paper in the form of frame-grabs. The view directions given for the images shown are calculated from the vehicle heading and the pan angle of the camera head. The absolute position of the vehicle relative to the ship was estimated using Posidonia (® IXSEA) Ultra-Short Baseline (USBL) navigation which has a theoretical positional accuracy of ±1% of water depth (in our study area ± 38 m). The vehicle also recorded its movements relative to the seafloor in one-second intervals using a doppler-velocity logger (DVL). These relative movements have much smaller, sub-centimeter, internal errors which, however, accumulate steadily over time.

Ship-based multibeam bathymetry was collected using a hull-mounted Kongsberg EM-122 system with 432 beams and a frequency of 12 kHz.

4. Results

4.1. Bathymetry

The ROV spent approximately 4.5 h on the seafloor (start 28.09.2015, 22:55UTC and end 29.09.2015, 03:35UTC) during dive 235ROV. Visual contact with the seafloor was maintained almost constantly and a video survey was carried out. A combined processing of the USBL and DVL navigation data (as described, for example, by Kwasnitschka et al., 2013) to determine the position of the vehicle during the dive proved to be very difficult as the area surveyed was small (ca. 200x500m) and so filtering to exclude spurious Posidonia fixes was unsuccessful. A bathymetric map for the survey is shown in Fig. 3, gridded at 6 m. It was constructed using the DVL data and the seafloor depth directly beneath the vehicle calculated from vehicle depth + altitude from 22:55 to 02:45, after which time the drift is estimated, based on geological observations on crossing video lines, to have become unacceptable for gridding purposes.

4.2. Geological observations

Several geological units can be identified visually on the ROV footage. These are described and illustrated in the following section. As direct sampling of the seafloor was not performed during this "search and rescue" ROV dive, any conclusions about the composition of the units are based solely on their appearance.

4.2.1. Linear scarps exposing sedimentary strata with overlying indurated layer

Several areas were seen with bedded sediments exposed along laterally continuous scarps. In all cases, these scarps could be followed in a relatively constant direction for many 10s of meters. The scarps all appear to be vertical - no sense of dip could be determined from the video footage.

Fig. 4A clearly shows the bedding in the sediments, which vary in colour from white to light grey/green and contain lighter-coloured inclusions which may be fossils - at the resolution of the video no identifcation is possible. In all cases, the sediment sequence is capped by a dark grey to black-coloured layer several centimeters thick (Fig. 4A, B & D) which in some cases extends as a flange or plate beyond the face of the sediment wall (e.g. Fig. 4B). Where well exposed, this cap layer can be seen to have an irregular and convoluted surface on the mm-cm scale, similar to surfaces reported for, for example, cobalt-rich crusts (see e.g., Halbach et al., 2017). Occasionally the sediment appears more massive and darker in colour and is cut by several parallel, steeply-dipping planes (see Fig. 4C). The exposed scarps show a variation of light to dark shades, with the base of the scarps (which are generally <5 m high, although one example ca. 20 m high was seen) always being lighter in colour.

More detailed examination of some of the scarps show rounded vertical channels in the sediments (Fig. 5). The channels are up to several 10s of cm across. It is notable that such channels are only seen in the sediments close to the scarps - on the flat sedimented areas away

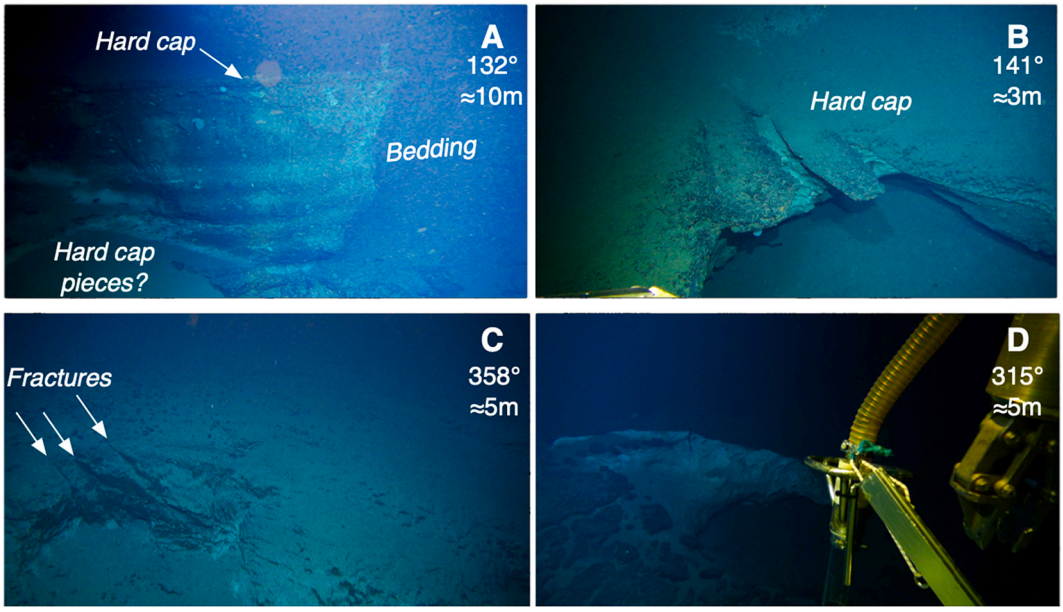

Fig. 4. Examples of bedded sediments exposed on scarps. All sediment sequences appear to have a hard cap (A–D), pieces of which are sometimes visible at the foot of the scarp (A, D). This cap is darker in colour than the sediments. The look direction (as degrees clockwise from North) of the photographs as well as the estimated horizontal width of the seafloor visible on the image is shown in the top right-hand corner.

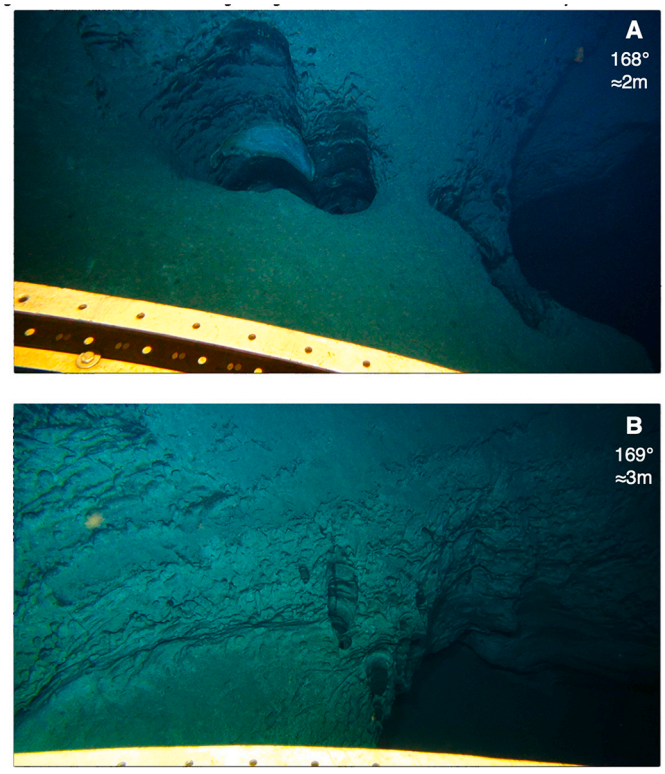

Fig. 5. Vertical channels running through the sediments. These channels are only seen near the cliffs - no depressions which could overlie such features are seen on flat sedimented surfaces. View directions and estimated scale indicated as in Fig. 4.

from the scarps, no "sink-holes" or similar features which might suggest underlying channels are visible.

4.2.2. Massive white sediment with dark veins

On the top of the shallow area in the northeast region of the dive area (see Fig. 3), outcrops of white sediments showing no discernible bedding are cut by veins of dark material. The dark veins are seen in places to have two raised margins and are associated with irregular clumps of dark material on the seafloor (see Fig. 6A). In close-up, the white sediment (Fig. 6B) shows signs of bioturbation (burrows are clearly seen), has a rounded, concoidal outcrop surface structure and is cut by numerous thin (1-2 mm), light-coloured, veinlets. Without samples it is not possible to determine whether the sediment is carbonate or silicic (but see discussion). The massive white sediment is cut on one side by a steep scarp littered with massive boulders with no pelagic sediment cover (Fig. 6C, D). On the scarp face itself, some dark patches are observed which look to consist of the same material as seen in the dark veins (Fig. 6E). We assume this is where the white sediment has broken along a vein, leaving some of the black material coating the surface. Some blocks of sediment entirely surrounded by veins are seen in one area (Fig. 6F).

4.2.3. Pillow lavas

The small east-west ridge in the western part of the dive area (see Fig. 3) appears to be constructed of pillow lavas and tubes (see Fig. 7) lying on top of dark, platy material similar to that seen on top of the sediments (see Section 4.2.1). The pillow lavas, which cover a region ca. 100x150m on a 10 m-high ridge, have only a thin dusting of unconsolidated sediment and occasional sessile organisms attached to them. Pillow tubes have the black colour, the longitudinal striations and other surface features and the 20-60 cm average diameter typical of basaltic pillow tubes seen elsewhere on the seafloor (e.g., Yeo et al., 2012). The area of the pillows was the only region during the dive where white decapods were observed (Fig. 7A). The pillows clearly lie on top of and are erupted through the dark platy material (Fig. 7B). The base of the pillow mound is marked by a sharp transition into underlying sediment (Fig. 7C).

4.2.4. White mounds

Two areas show small, white mounds protruding several 10s of cm above the seafloor. These constructs are seen both at the base of the pillow ridge (Fig. 8A) and associated with the dark veins in the massive white sediment (Fig. 8B). The mound in Fig. 8A appears to be surrounded by a lighter-coloured halo on the adjacent seafloor. These

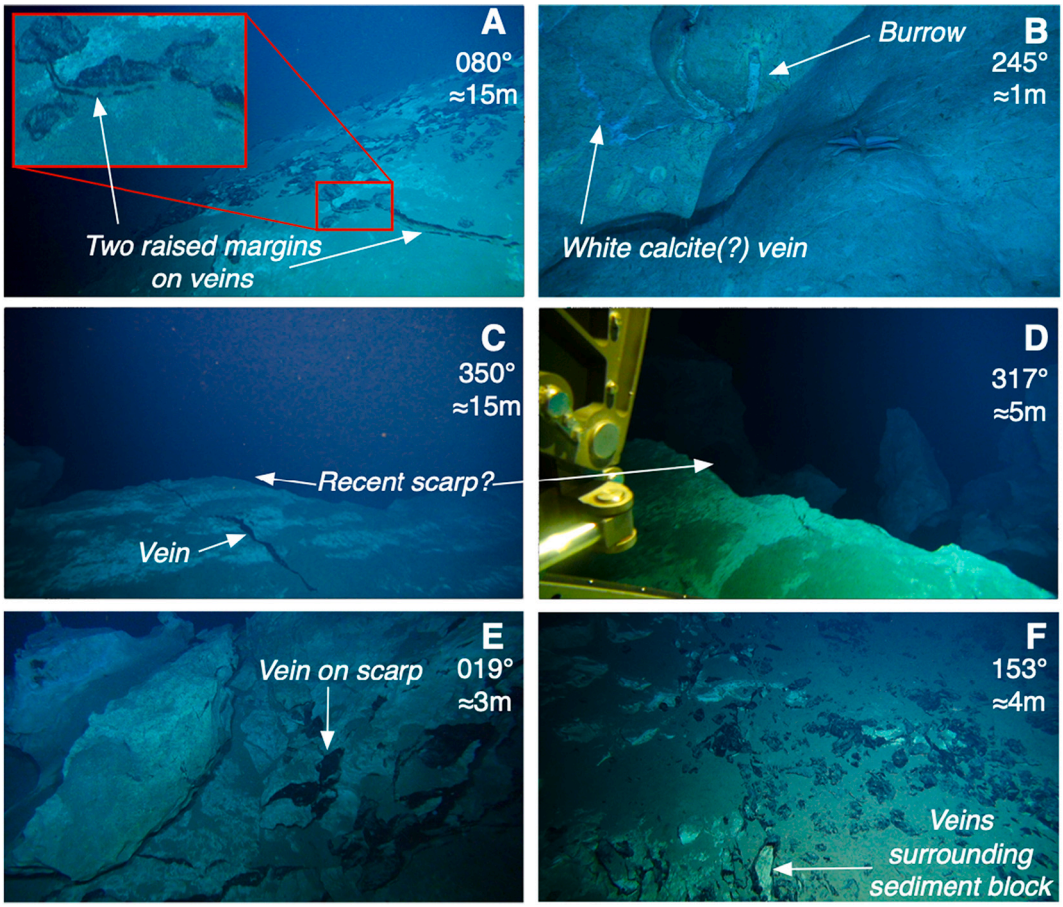

Fig. 6. Dark veins running through white sediment on the seafloor. (A) The veins show two raised margins and are associated with clumps of dark material on the surrounding seafloor. (B) The white sediment is massive, shows concoidal surface structure and is cut by thin white veins. (C) A dark vein terminates at a scarp. (D) The boulders below the scarp are angular and show little sediment dusting. (E) On the scarp the dark veins are seen coating surfaces in the white sediment. (F) Dark veins completely surrounding blocks of sediment, note also the zonation in proportion of sediment to veins from left (few veins) to right (vein dominated) across the picture. View directions and estimated scales as in Fig. 4.

mounds show no sign of biological activity on their surface and appear to be located on both soft (Fig. 8A) and hard (Fig. 8B) substrate.

5. Discussion

5.1. Geological interpretation of rock types

Beside the pillow lavas, several different lithologies are evidently present in the dive area. Although no samples were collected, the video information provides numerous indications of what these lithologies may be:

- *Sediments*: Both grey-green and white sediments are seen on the small seamount. In view of the higher content of carbonate relative to opal in present-day sediment being deposited at this location in the Peru Basin (Lyle, 1992) and the fact that, over the 20 Ma since this crust formed, seafloor depth will have been shallower than it presently is and so more amenable to carbonate conservation, we feel it is most likely that most of the sediments we observe, and especially those showing a white colour, are carbonates. The dark indurated cap seen on the grey-green sediments in places is reminiscient of Mn-crusts reported from seamounts throughout the Pacific (e.g., Segl et al., 1984)
- *Dark veins*: The nature of the black veins which cut the white sediments is difficult to determine from photographic evidence alone. The material must, at some stage, have been in a liquid form to fill the veins, and so either was itself a liquid or its material was deposited from flowing fluid. Several black, mobile materials can occur on the seafloor, especially lava, asphalt and manganese-containing solutions. The absence of chemosynthetic organisms colonizing the veins suggests that the material is not asphalt (c.f. Marcon et al., 2018). The matte appearance of the veins on exposed surfaces (e.g., Fig. 6E) could imply a manganese oxide coating (magmatic intrusions might be expected to show shiny, glassy surfaces) but the presence of large surface accumulations of black material (Fig. 6A inset, Fig. 6F) next to the veins seems incompatible with Mn-oxide deposition from a solution. So a magmatic origin for the veins seems most likely.
- *White mounds*: The shape and colour of the white mounds shown on Fig. 8 does not appear to conform to any known deep-sea animal group and we conclude that they are geological rather than biological constructs. Although the video information shows no signs of active fluid venting, these features are clearly constructed above the seafloor and have some rigidity (i.e. they are not merely mounds of loose material) leading us to the conclusion that they may be constructed from mineral precipitation around the exit points of crustal fluid (i.e., they are “chimneys”).

5.2. A geological map of the seamount

Assuming these rock type classifications are correct, the video observations, combined with the vehicle position, can be used to produce a geological map of the dive area, which is shown in Fig. 9. On this map, boundaries which lie directly on the ROV track (shown by the depth-

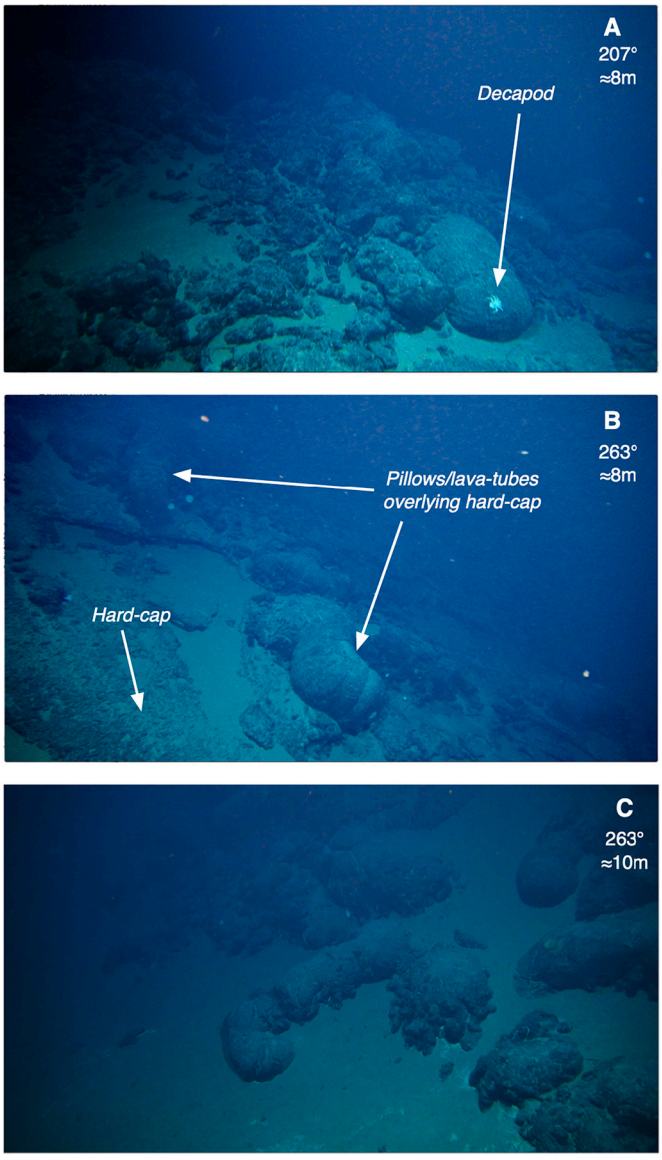

Fig. 7. Young pillows on old seafloor. (A) Near the summit of the pillow mound. (B) Pillow flows emerge through a hard-cap which appears very similar to that seen elsewhere on the top of the uplifted sediment blocks (see e.g. Fig. 4A). (C) The sedimented basal contact of the pillow ridge. View directions and estimated scales as in Fig. 4.

coded track) are located based on direct observations and have the highest confidence. Between the ROV tracks, where there are no observations, boundaries have been extended in what appears to us to be the most logical configuration, similar to procedures used in field geological mapping on land. In regions where the ROV tracks are widely spaced, the location of these interpolated boundaries will be subject to large errors. With an estimated field of view from the ROV of up to 10 m (this varied during the dive due to the ROV occassionally stirring up sediment from the seafloor, reducing visibility. Also in the region of the pillow mound the visibility appeared to be somewhat reduced), in regions with closely spaced ROV tracks the boundaries are much better constrained.

There are several features of the rock types and their relationships to each other shown on this map which imply that this region of the Peru Basin, normally thought of as an inactive intraplate area, has experienced relatively recent magmatism, possibly associated with local tectonic activity:

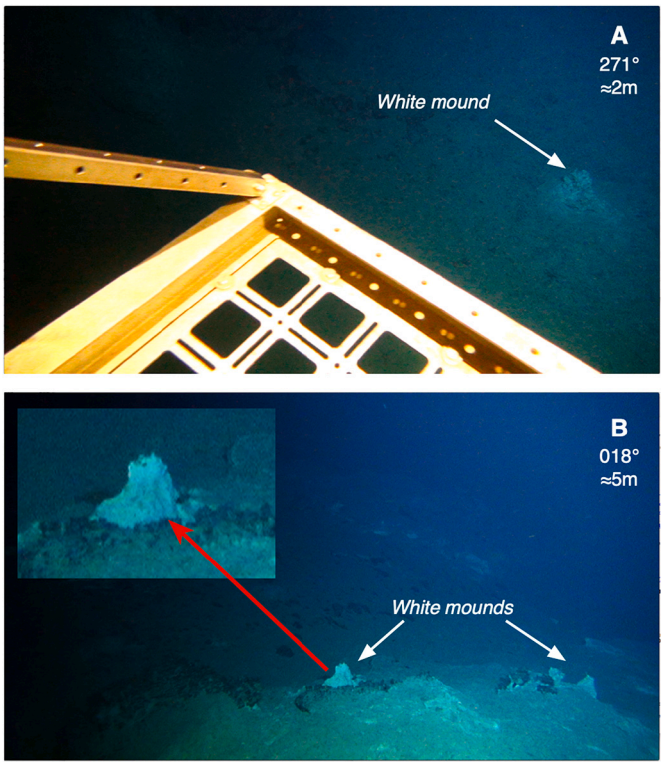

Fig. 8. White mound structures. (A) a white mound located on sediment at the base of the pillow mound. The ROV "porch" is visible in the lower part of the picture. (B) White mounds located along one of the dark veins described above (see also Fig. 6). The blow-up shows the irrgular and steep shape of the mound. View directions and estimated scales as in Fig. 4.

1. Most of the seamount summit region surveyed during the ROV deployment is covered in grey/green deep water sediments, similar to those seen in the adjacent DISCOL nodule area (see Cruise Report SO242-1; Greinert, 2015). Evidence from the bedded sediments exposed in the scarps (Fig. 4) suggests that this type of sedimentation has been occurring on this seamount for extensive periods (no magmatic basement was seen exposed below the sediment on any of these scarps). Such scarps could be the result of either tectonic reactivtion or mass-wasting, although their linear nature suggests the former is more likely. As they expose indurated sediment showing no sign of slumping (and indeed occasionally the scarps are overhanging, see Fig. 4A) we conclude that the scarps were formed post-diagenetically. During the SO242/2 cruise, Parasound sub-bottom profiling data (Grant and Schreiber, 1990) were collected along several tracks (see fig. 7.1.2 in Boetius (2015)) from which data (https://doi.org/10.1594/PANGAEA.854122) and images (https://doi.org/10.1594/PANGAEA.854124) are freely available online. Two tracks passed over the seamount studied here, between 20:40 and 21:40 UTC on 13 Sept. 2015 (image SO242_2_192_01_SLF) and 03:10–04:00 UTC on 5 Sept. 2015 (image SO242_2_161_SLF). Both passes show Parasound records typical for steep-sided features, with little sub-bottom penetration and multiple parabolic side-echoes. In the few instances when penetration was achieved (e.g., between 20:55 and 21:00 on 13 Sept 2015) the image shows >10 m of undisturbed bedded sediment on the seamount flank and did not reach acoustic basement. The flatter seafloor around the seamount shows more consistent penertration of up to 50 m and also parallel-bedded, apparently undisturbed sediments, the acoustic basement was here also not reached.
2. The scarps have two main orientations, roughly N-S and E-W (see Fig. 9). These orientations are relatively well constrained either by repeated crossings with the ROV (the most easterly and westerly

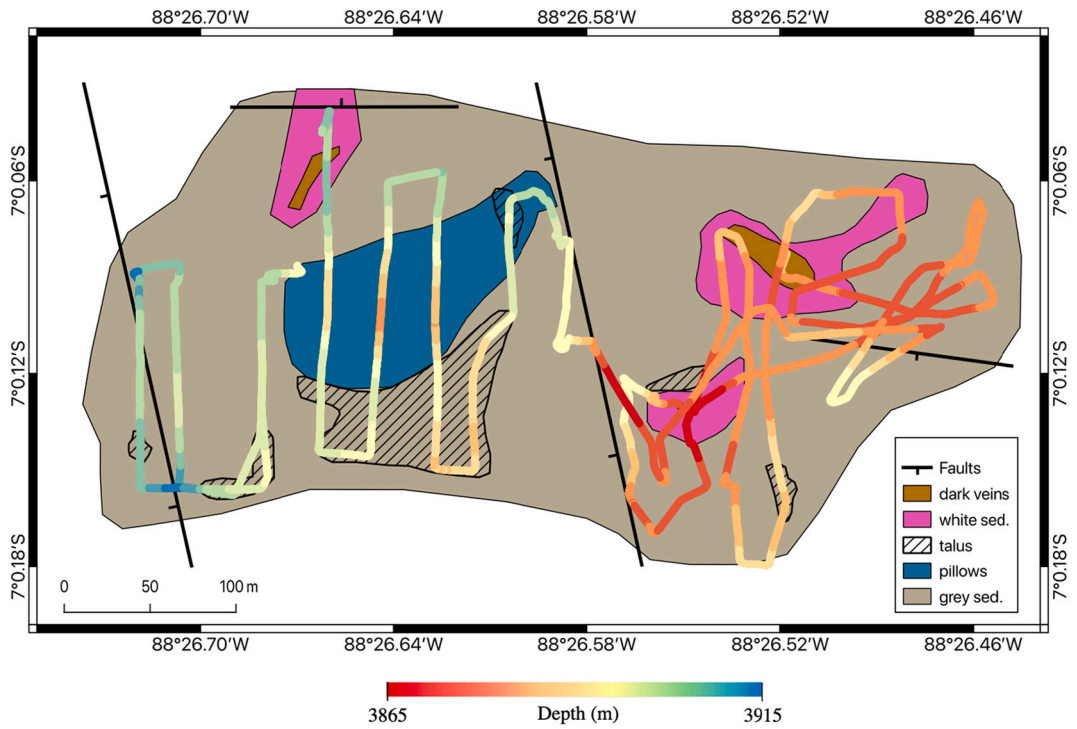

Fig. 9. Geological map of the dive area on the summit of the volcano shown on Fig. 2. The coloured track shows the water depth using the same data and colour scale as for Fig. 3. Tick marks on the lines marking the scarps show their down-step side.

scarps) or because the ROV-trajectory approximately followed the scarp, keeping it in view for some distance (the more easterly of the two N-S-running scarps). The N-S-trending scarps both down-step to the west, separating the summit into two platforms. We interpret these scarps as being the traces of faults on the seamount summit although we found no evidence to prove this unequivocally. The more easterly platform, which includes the shallowest bathymetry in the area and is centred on 88°26.52′W (Fig. 3), is characterized by the white, unbedded sediments crosscut by dark veins (Fig. 6), although a patch of similar sediments is also seen to the north of the pillow ridge on the western block (see locations of Fig. 6C–E on Fig. 3). The lack of distinguishable bedding in these white sediments combined with their concoidal outcrop surface implies that they have experienced more induration/diagenesis than the greenish bedded sediments seen elsewhere. The occurrence of cross-cutting white veins in the sediments may even imply that they have begun to be remobilised and may be more fittingly described as marbles rather than sediment.

3. The marbles are cross-cut by dark, presumably magmatic veins which are occassionally surmounted by small white chimneys. None of the exposures shows more than a thin sediment dusting, suggesting that they formed in their present configuration relatively recently. The veins occasionally show raised margins (Fig. 6A) which may represent chilled margins. Our preferred interpretation for these outcrops is that the white host sediments have suffered contact metamorphism in proximity to a magma body and that the dark veins are thin dykes of this magma intruding the sediments.
4. The western platform shows more conventional pillow-volcano magmatism. As with the veins and chimneys, the pillow lavas show little sediment cover (Fig. 7), again suggesting that they are relatively recent eruptions (although with sedimentation rates in this region being relatively low (1–10 mm/kyr, e.g., Marchig and Reyss, 1984) it is difficult to determine their exact age). This is supported by the presence of crustaceans, which on the videos resemble the munidopsis "squat lobsters" (*Munidopsis subsquamosa* Henderson), on these pillows - such animals are often (although not exclusively) found near hydrothermal vents (e.g., Chadwick et al., 2018; Macpherson and Segonzac, 2005). The amount of extrusive volcanism appears to be very minor - Fig. 7B shows individual pillow tubes resting on what appears to be the Mn-crust normally seen topping the sediment pile (e.g. Fig. 4). This crust appears to have been fractured and bent upwards, presumably by underlying, intruding magma.

Independent corroboration for the occurrence of recent volcanic and tectonic activity on and around the seamount comes from two sources: Firstly, in 1992 Marchig et al. (1999) carried out a photo-sled profile over the volcano (the exact path the sled took can, unfortunately, no longer be determined) and report detecting spiked temperature anomalies of almost 0.1 °C in the water column above the volcano (see their Fig. 3). They took this as strong evidence that the volcano was young and still hydrothermally active. And secondly, in 2 October 1988 a magnitude 4.7 earthquake was detected teleseismically in the area and assigned a location (7.065°S/88.619°W, see Fig. 1) ca. 25 km west of the seamount and a shallow depth of 10 km (IRIS catalogue, event timestamp 591,837,663). In view of the errors inherent in teleseismic epicentre relocation, this earthquake occurred within error of the seamount studied here.

Taken together, the evidence for pillow lavas lying on top of Mn-crusts shown here combined with temperature anomalies in the water column reported by Marchig et al. (1999) would seem to be enough to conclude that active volcanism is occurring on this 20 Ma crust. Although the volcano studied here is relatively small, its location in the middle of the Peru Basin, an area expected, in plate tectonics, to have been tectonically and volcanically inactive for many millions of years, is unusual. This led us to search for other evidence of volcanism in the area.

5.3. *Regional plate tectonic setting and possible triggers for DISCOL volcanism*

In Section 1 we listed several phenomena (hotspots, petit-spots, mantle convective rolls or intraplate stress) which have previously

been advanced as causes of intraplate volcanism. It is instructive to evaluate whether any of these could be responsbile for the small-volume intraplate volcanism we observe.

A compilation of hotspot locations (Steinberger, 2000) shows no known hotspot in the vicinity of the DISCOL area, the nearest is Galapagos at >600 Km, the other Nazca Plate hotspots (Easter, Juan Fernandez, San Felix) are all >2000 km distant. Although work in the Atlantic (Long et al., 2020) has suggested that plume material may contaminate the upper mantle over distances of several hundred km and lead to dispersed volcanism near major plumes, the edifices they sampled were all large constructive features (some apparently former islands which had been eroded to guyots) unlike the DISCOL volcano we study here. Additionally, Long et al. (2020) postulated that the contamination was linked to a spreading head of material from the Canary and/or Cape Verde plume stalled at around 1000 km depth in the mantle over 60 Ma ago and visible in seismic tomography images. The Galapagos plume shows no such deep root (French and Romanowicz, 2015; French and Romanowicz, 2014) and so is unlikely to be a potential source for such plume contamination.

The work on petit-spots has shown them to be mechanistically linked to plate flexure prior to subduction, as all petit-spot volcanoes are found either on the concavely-deforming outer regions of the outer rise or on the convexly flexured crest of the outer rise itself (Hirano, 2011; Hirano et al., 2001; Hirano et al., 2013; Hirano et al., 2006; Sato et al., 2018). The deformation of Atlantic lithosphere south of Greenland as a result of glaciation/de-glaciation cycling has also been proposed to explain the formation of a large (110 km long) un-named magmatic ridge there. Once more, the unexceptional seafloor depth of the DISCOL region, which lies on the age-depth curve for lithospheric cooling, suggests it is not involved in such flexural tectonics. The DISCOL region is also much further from the South American trench (600 km) than the locations suggested by Hirano et al. (2013) to have experienced petit-spot volcanism due to flexure off Chile (ca. 250 km). We do not, therefore, attribute the DISCOL volcanism to a petit spot origin.

Two large linear volcanic ridges (the Alvarado and Sarmiento Ridges, see Fig. 1) are present on the Nazca plate. Little is known about their activity and no radiometric ages or geochemical analyses have been published. Lonsdale (2005), in the only publication to discuss their origin, concluded (based on "a few traverses of bathymetric data" and the fact that they did not offset magnetic anomalies) that they were not linked to fracture zones but instead "closely resemble the linear volcanic ridges built over eruptive fractures that extend down the young flanks of active eastern Pacific rises, such as Sojourn Ridge on the Pacific–Nazca EPR". The Sojourn Ridge extends between 50 and 550 km to the west of the EPR and is younger than the underlying crust by up to 5 Ma (Forsyth et al., 2006). Lonsdale (2005) notes that the Alvarado and Sarmiento Ridges extend westward from the trench to EPR crustal ages of ca. 25 Ma, meaning that if their origin is similar to Sojourn Ridge they will have been inactive for the last 20 Ma. Evidence that such off-axis linear ridges do at some distance from the ridge cease to be active comes from the Puka Puka ridge which, although extending up to 2000 km across the Pacific plate from the EPR, is known to be inactive in all but its most near-ridge part (Forsyth et al., 2006). We note additionally that the DISCOL region is not in line with either the Alvarado or the Sarmiento Ridges and that a characteristic feature of the off-axis ridges such as Sojourn or Puka Puka is their elongated form and constant direction over many hundreds of kilometers.

Evidence for plate extension and cracking in response to far-field (plate tectonic) or within-plate thermal contraction stresses as a cause or focusser of intraplate volcanism has been sought in many places. Sandwell and Fialko (2004) suggested that cooling and contraction of the Pacific Plate was responsible for lineaments in the gravity field associated with the Sojourn, Puku Puka etc. Ridges, although Forsyth et al. (2006) failed to find any evidence for it in the field and found that even young, small volcanoes did not appear to be associated with lineation-parallel cracks or graben in the plate. Cormier et al. (2011), studying the Cocos Plate, found that the gravity lineations there were perpendicular to crustal isochrons and suggested that this was evidence for thermal contraction. In the Peru Basin region studied here, no evidence has been presented in the literature to suggest the plate may be experiencing extension and no earthquake centroid moment tensor solutions for the few intraplate earthquakes which have been detected (see Fig. 1) are available. In the DISCOL study area itself, extensive and detailed studies of the seafloor, including deep-submergence side-scan sonar and photomosaics (e.g., Gausepohl et al., 2020), have not shown any signs of active tectonic lineaments at the seafloor which might reflect recent extensional tectonics there.

So what might be the cause of the DISCOL volcanism? The tomographic model of French and Romanowicz (2014) shows the whole Nazca plate to be underlain by slow Vs signatures at shallow (70 km) depth (see their Fig. 8, SEMUCB_WM1 slice at 70 km). The lateral extent of these slow anomalies (over 4000 km) appears globally exceptional when compared to other regions of the spreading system, where slow Vs anomalies extend at most only 200-300 km off-axis (see e.g., Toomey et al., 1998). This may indicate that the Nazca plate (and large areas of the conjugate part of the Pacific plate) is underlain by mantle with an elevated magma content. The seafloor on which the DISCOL volcano sits has been described as having been generated either (i) at the now-extinct Galapagos Rise (Marchig et al., 1999) which at the time was the boundary between the Bauer microplate (Mammerickx et al., 1980) and the Nazca plate or (ii) at the East-Pacific Rise (Lonsdale, 2005; Meschede et al., 2008; Meschede et al., 1998). A detailed study of the Bauer microplate and its overlapping spreading axes (Eakins and Lonsdale, 2003) clearly shows that crust created at the Galapagos Rise does not extend further east than ca. 90°W at a latitude of 12–13°S and that at the latitude of the DISCOL volcano (7°S) the Galapagos Rise crust does not extend eastward of ca. 97°W. This make the crust on which the DISCOL volcano sits clearly of EPR origin.

In view of the fact that seafloor depths in the DISCOL region are as expected from the seafloor age, we conclude that the Vs anomaly at 70 km depth is not related to higher-than-normal mantle temperatures but may instead reflect a higher proportion of incipient or residual melt in the mantle, possibly related to increased fertility. We suggest that it is this melt which has fed the volcano studied here, although geochemical analysis of samples from the volcano would be required to definitely support or reject this hypothesis. Marchig et al. (1999) did not sample the small volcano we have studied here but concluded, based on their geochemistry, that samples dredged from the two small seamounts to the NW and W (labelled M. and W&W on Fig. 1, see also discussion in Section 5.4) had ocean island basalt affinities as they classified as alkali basalts on a total alkali/silica diagram and showed elevated La/Lu ratios.

If the volcanism we report is related to the Vs anomaly which appears to be present under large areas of the Nazca plate, we might expect to find similar volcanoes occurring elsewhere in the region. Although investigations of the type reported here have not been carried out at other sites, some evidence for additional volcanism in the region is available.

5.4. Other signs of recent volcanism in the region

Modern multibeam sonar systems are capable of recording the acoustic backscatter intensity in addition to the water depth information. In areas such as the one studied here, which are far from plate boundaries and so should be heavily sedimented, the difference in acoustic backscatter between hard, rough volcanic rocks and deep-sea sediment makes recent volcanic constructs easily detectable. Fig. 10 shows the bathymetry and co-registered backscatter intensity (high intensity = light colour) for a region east and north of the DISCOL area (the region covered by this figure on shown on Fig. 1). Note that the effects of grazing angles on the backscatter intensity were corrected (using the co-registered bathymetric information) during processing with the program FMGT from the "Fledermaus" suite produced by QPS.

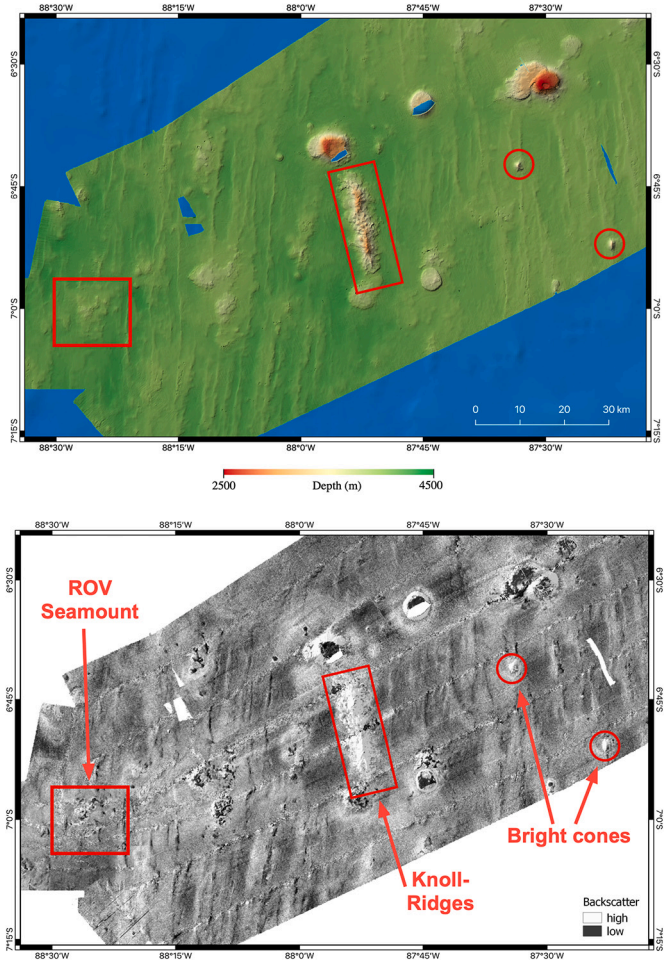

Fig. 10. Regional bathymetry (top) and acoustic backscatter intensity (bottom) information for the vicinity of the DISCOL area. The features referred to in the text are labelled on the backscatter map and outlined in red on the bathymetric map. (For interpretation of the references to colour in this figure legend, the reader is referred to the web version of this article.)

The small, relatively young pillow mound whose ROV-exploration has been discussed here ("ROV Seamount"), with an overall dimension estimated at 150x100m (see Fig. 3), is below the detection limit at the calculated grid cell size of 80 m and thus is not evident on Fig. 10. Several other features do, however, stand out. Approximately 50 km to the ENE of the ROV seamount, two N-S orientated ridges with a rugose form covered in knolls (labelled "Knoll-Ridges" on Fig. 10) are visible in both the bathymetric and backscatter maps. The general higher backscatter and the complicated surface shape of the ridges suggest that they are relatively unsedimented volcanic structures. Thirty kilometers east of the Knoll-Ridges are two conical features ("Bright cones") also showing high backscatter. These seamounts rise more than 600 m above the surrounding seafloor and the high backscatter intensities are seen even on slopes facing away from the ship, implying that their high reflectivity is not the result of errors in the grazing-angle corrections. Other than the maps presented here, we unfortunately have no information on the geology of the Knoll-Ridges or Bright Cones - they represents prime targets for future exploration of volcanism on old Pacific seafloor.

Although the region has never been the focus of a systematic search, two other indications of young, intraplate volcanism in the Peru Basin can be found in the literature. Thus, for example, Marchig et al. (1999) present information on hydrothermal activity in the Peru Basin for which they collected sediment, Mn-nodule and rock samples from two regions west and north of the DISCOL area. During their work they identified a large seamount at 6°25′S/90°45′W rising 2000 m above the surrounding seafloor (marked "M." on Fig. 1) from which they recovered alkali basalt samples. Oxygen isotope stratigraphy on a sediment core taken adjacent to this large seamount suggests volcanism occurred there at ca. 5 Ma, between 10 and 15 Ma after the crust was created. Wiedicke and Weber (1996), examining acoustic records from the same cruise, found deep-towed side-scan sonar evidence for small volcanoes "nearly free of sediment" in a region near 8°35′S/90°45′W (marked "W&W" on Fig. 1) which they concluded may be Quaternary in age.

The region studied here has also not been the subject of extensive heat-flow work, with the global compilation of heat-flow measurements assembled by the IASPEI/IAVCEI/IAGA/IAPSO/IAMAS/IAHS "International Heat Flow Commission" (https://ihfc-iugg.org/products/global-heat-flow-database) providing only three values from the general region (values shown and positions marked by circles on Fig. 1). The scatter on these values, at 319, 16 and 60 mW/m^2, is far beyond what would be expected for a 20 Ma oceanic plate (theoretical value ≈ 100, observational mean ≈ 70 and observational range ≈20–180: Hasterok et al., 2011), indicating that the heat-flow regime in this part of the seafloor is not purely conductive and that advective heat transport, either from magmatism or fluid circulation in the crust, is probably occurring.

5.5. Global implications

To what extent the evidence of scattered young volcanism on old Nazca Plate seafloor shown here is representative for the abyssal seafloor globally is impossible to assess at present. The necessary acoustic surveys in abyssal regions coupled with the kind of deep-submergence investigations we have presented have simply not been performed. But even within the confines of the Nazca Plate itself, our findings have important consequences which go beyond marine geology. The dispersal of vent-associated chemosynthetic organisms is thought to be controlled by the availability of sufficiently closely-spaced habitats for larvae to colonize (e.g., Van Dover et al., 2001) but several studies (e.g., van der Heijden et al., 2012) have shown, using genetic markers in geographically widely seperated populations, that physical barriers to migration appear to be relatively unimportant, suggesting that more hydrothermal springs are present on the seafloor than detected by water-column surveys for hydrothermal plume effluent (Breusing et al., 2016). Small intraplate volcanoes such as those investigated here could, if present over wide areas, provide the solution to this conundrum, providing oases for life on the supposedly barren abyssal plain.

6. Conclusions

An examination of ROV video from a seamount on 20 Ma crust in the Peru Basin, combined with regional ship-based bathymetric and acoustic backscatter data on the Nazca Plate, leads to the following conclusions:

- Most of the seafloor at the summit of the seamount is covered in thick, consolidated sediment as might be expected for a 20 Ma-old seamount. Sections through this sediment exposed on fault scarps (up to 20 m high) and acoustic sub-bottom profiles do not reach deep enough to detect underlying igneous basement.
- Small areas of the seamount summit show evidence for magmatism. All magmatic exposures show only a light dusting of sediment with no continuous sediment blanket being seen, suggesting they are much younger than the rest of the seamount.
- Magmatism has produced a small (ca. 100x150m in area, ca. 10 m high) pillow mound and also veins and dykes in the sediments. The intrusions appear to have metamorphosed the adjacent carbonate sediments.
- The occurence of several small chimneys, some clearly associated with the dykes, and the presence of what is possibly a *munidopsis*

squat lobster on the pillows both suggest that the seamount may be presently hydrothermally active, although no active venting was seen. This is confirmed by temperature anomalies in the water column over the seamount seen in 1992.

- Regionally, we see other indications for recent volcanism and disturbed heat-flow, implying that this intraplate region is still volcanically active.

Data Availability

The data presented and/or discussed in this paper are available from the following sources: Raw multibeam data cruise SO242/1: Greinert (2016) URL:https://doi.pangaea.de/10.1594/PANGAEA.859528 Raw multibeam data cruise SO242/2: Boetius and Roessler (2015a,b,c) URL https://doi.org/10.1594/PANGAEA.854125 Gridded bathymetric data from the DISCOL area used for Fig. 2: Gausepohl et al. (2019) URL https://doi.org/10.5194/bg-17-1463-2020 Parasound bottom-penetrating sonar data and images: Boetius and Roessler (2015a, 2015b) URL https://doi.org/10.1594/PANGAEA.854124 and https://doi.org/10.1594/PANGAEA.854122.

Declaration of Competing Interest

The authors declare that they have no known competing financial interests or personal relationships that could have appeared to influence the work reported in this paper.

Acknowledgements

The JPI-OCEANS cruises were funded by the German Science Ministry BMBF (Bundesministerium für Bildung und Forschung) as part of the European Horizon2020 Joint Programming Initiative. ROV "Kiel6000" is maintained and operated with funding from the Helmholtz Association via GEOMAR. C. Melchior is thanked for help compiling Fig. 1. Michael Riedel provided insightful comments on the SO242/2 Parasound data. We thank Bill Chadwick and several anonymous reviewers for detailed and insightful reviews which repeatedly led to significant improvements in the manuscript.

References

Ballmer, M.D., Conrad, C.P., Smith, E.I., Harmon, N., 2013. Non-hotspot volcano chains produced by migration of shear-driven upwelling toward the East Pacific Rise. Geology 41, 479–482.

Boetius, A.E., 2015. RV SONNE Fahrtbericht/Cruise Report SO242-2 [SO242/2]: JPI OCEANS Ecological Aspects of Deep-Sea Mining, DISCOL Revisited, Guayaquil - Guayaquil (Equador), 28.08.-01.10.2015, GEOMAR Report, N. Ser. 27. GEOMAR Helmholtz-Centre for Ocean Research Kiel, Kiel (552 pp).

Boetius, A., Roessler, S., 2015a. Profile of sediment echo sounding during SONNE cruise SO242/2 (DISCOL) in the Peru Basin, South Pacific Ocean, with links to images. pangaea.de. https://doi.org/10.1594/PANGAEA.854124.

Boetius, A., Roessler, S., 2015b. Profile of sediment echo sounding during SONNE cruise SO242/2 (DISCOL) in the Peru Basin, South Pacific Ocean, with links to ParaSound. pangaea.de. https://doi.org/10.1594/PANGAEA.854122.

Boetius, A., Roessler, S., 2015c. Swath sonar multibeam EM122 bathymetry during SONNE cruise SO242/2 (DISCOL) in the Peru Basin, South Pacific Ocean, with links to raw data files. pangaea.de. https://doi.org/10.1594/PANGAEA.854125.

Borowski, C., Thiel, H., 1998. Deep-sea macrofaunal impacts of a large-scale physical disturbance experiment in the Southeast Pacific. Deep-Sea Res II Top. Stud. Oceanogr. 45, 55–81.

Breusing, C., Biastoch, A., Drews, A., Metaxas, A., Jollivet, D., Vrijenhoek, R.C., Bayer, T., Melzner, F., Sayavedra, L., Petersen, J.M., Dubilier, N., Schilhabel, M.B., Rosenstiel, P., Reusch, T.B.H., 2016. Biophysical and population genetic models predict the presence of "phantom" stepping stones connecting mid-atlantic ridge vent ecosystems. Curr. Biol. 26, 2257–2267.

Castillo, P.R., Lonsdale, P.F., 2004. Geochemistry of Alvarado and Sarmiento Ridges Suggests Widespread Galapagos Plume-Upper Mantle Interaction in the Miocene Eastern Pacific?, AGU Fall Meeting. AGU, San Francisco.

Chadwick, W.W.J., Merle, S.G., Baker, E.T., Walker, S.L., Resing, J.A., Butterfield, D.A., Anderson, M.O., Baumberger, T., Bobbitt, A.M., 2018. A recent volcanic eruption discovered on the central Mariana back-arc spreading center. Front. Earth Sci. 6.

Cormier, M.-H., Gans, K.D., Wilson, D.S., 2011. Gravity lineaments of the Cocos Plate: Evidence for a thermal contraction crack origin. Geochem. Geophys. Geosys. 12 (7) https://doi.org/10.1029/2011GC003573.

Drazen, J.C., Leitner, A.B., Morningstar, S., Marcon, Y., Greinert, J., Purser, A., 2019. Observations of deep-sea fishes and mobile scavengers from the abyssal DISCOL experimental mining area. Biogeosciences 16, 3133–3146.

Eakins, B.W., Lonsdale, P.F., 2003. Structural patterns and tectonic history of the Bauer microplate, Eastern Tropical Pacific. Mar. Geophys. Res. 24 (3–4), 171–205. https://doi.org/10.1007/s11001-004-5882-4.

Forsyth, D.W., Harmon, N., Scheirer, D.S., Duncan, R.A., 2006. Distribution of recent volcanism and the morphology of seamounts and ridges in the GLIMPSE study area: Implications for the lithospheric cracking hypothesis for the origin of intraplate, non-hot spot volcanic chains. J. Geophys. Res. Solid Earth 111.

French, S.W., Romanowicz, B.A., 2014. Whole-mantle radially anisotropic shear velocity structure from spectral-element waveform tomography. Geophys. J. R. Astron. Soc. 199, 1303–1327.

French, S.W., Romanowicz, B., 2015. Broad plumes rooted at the base of the Earth's mantle beneath major hotspots. Nature 525, 95.

Gausepohl, F., Hennke, A., Schoening, T., Koeser, K., Greinert, J., 2020. Scars in the abyss: reconstructing sequence, location and temporal change of the 78 plough tracks of the 1989 DISCOL deep-sea disturbance experiment in the Peru Basin. Biogeosciences 17, 1463–1493.

Gausepohl, F., Hennke, A., Schoening, T., Köser, K., Greinert, J., 2019. Bathymetric grid from the DISCOL working area of SONNE cruise SO242/1 in the Peru-basin. pangaea.de. https://doi.org/10.5194/bg-17-1463-2020.

Grant, J.A., Schreiber, R., 1990. Modern swathe sounding and subbottom profiling technology for research applications – the Atlas hydrosweep and parasound systems. Mar. Geophys. Res. 12, 9–19.

Greinert, J.E., 2015. Cruise Report SO242-1: JPI OCEANS Ecological aspects of deep-sea mining, DISCOL revisited. In: Guayaquil - Guayaquil (Equador) 28.07–25.08.2015, GEOMAR Report, N. Ser. 26. GEOMAR Helmholtz-Centre for Ocean Research Kiel, Kiel, Germany (290 pp).

Greinert, J., 2016. Swath sonar multibeam EM122 bathymetry during SONNE cruise SO242/1 with links to raw data files. pangaea.de. https://doi.org/10.1594/PANGAEA.859528.

Haase, K.M., Devey, C.W., 1994. The petrology and geochemistry of Vesteris Seamount, Greenland basin – an intraplate alkaline volcano of non-plume origin. J. Petrol. 35, 295–328.

Halbach, P.E., Jahn, A., Cherkashov, G., 2017. Marine co-rich ferromanganese crust deposits: description and formation, occurrences and distribution, estimated world-wide resources. In: Sharma, R. (Ed.), Deep-Sea Mining. Springer, Cham.

Harigane, Y., Mizukami, T., Morishita, T., Michibayashi, K., Abe, N., Hirano, N., 2011. Direct evidence for upper mantle structure in the NW Pacific Plate: microstructural analysis of a petit-spot peridotite xenolith. Earth Planet. Sci. Lett. 302, 194–202.

Hasterok, D., Chapman, D.S., Davis, E.E., 2011. Oceanic heat flow: implications for global heat loss. Earth Planet. Sci. Lett. 311, 386–395.

Hirano, N., 2011. Petit-spot volcanism: a new type of volcanic zone discovered near a trench. Geochem. J. 45, 157–167.

Hirano, N., Kawamura, K., Hattori, M., Saito, K., Ogawa, Y., 2001. A new type of intra-plate volcanism; young alkali-basalts discovered from the subducting Pacific Plate, northern Japan Trench. Geophys. Res. Lett. 28, 2719–2722.

Hirano, N., Takahashi, E., Yamamoto, J., Abe, N., Ingle, S.P., Kaneoka, I., Hirata, T., Kimura, J.-I., Ishii, T., Ogawa, Y., Machida, S., Suyehiro, K., 2006. Volcanism in response to plate flexure. Science 313, 1426–1428.

Hirano, N., Machida, S., Abe, N., Morishita, T., Tamura, A., Arai, S., 2013. Petit-spot lava fields off the central Chile trench induced by plate flexure. Geochem. J. 47, 249–257.

Holmes, R.C., Webb, S.C., Forsyth, D.W., 2007. Crustal structure beneath the gravity lineations in the Gravity Lineations, Intraplate Melting, Petrologic and Seismic Expedition (GLIMPSE) study area from seismic refraction data. J. Geophys. Res. Solid Earth Planets 112, B07316. https://doi.org/10.1029/2006JB004685.

Korenaga, T., Korenaga, J., 2008. Subsidence of normal oceanic lithosphere, apparent thermal expansivity, and seafloor flattening. Earth Planet. Sci. Lett. 268, 41–51.

Kwasnitschka, T., Hansteen, T.H., Devey, C.W., Kutterolf, S., 2013. Doing fieldwork on the seafloor: photogrammetric techniques to yield 3D visual models from ROV video. Comput. Geosci. 52, 218–226.

Long, X., Geldmacher, J., Hoernle, K., Hauff, F., Wartho, J.-A., Garbe-Schoenberg, C.D., 2020. Origin of isolated seamounts in the Canary Basin (East Atlantic): the role of plume material in the origin of seamounts not associated with hotspot tracks. Terra Nova 32, 390–398.

Lonsdale, P., 2005. Creation of the Cocos and Nazca plates by fission of the Farallon plate. Tectonophysics 404, 237–264.

Lyle, M., 1992. Composition maps of surface sediments of the eastern tropical Pacific Ocean. In: Mayer, L.A., Pisias, N., Janecek, T., et al. (Eds.), Proceeding of the Ocean Drilling Program, Initial Reports. (Ocean Drilling Program), College Station, TX, pp. 101–115.

Macpherson, E., Segonzac, M., 2005. Species of the genus Munidopsis (Crustacea, Decapoda, Galatheidae) from the deep Atlantic Ocean, including cold-seep and hydrothermal vent areas. Zootaxa 3–60.

Mammerickx, J., Herron, E., Dorman, L., 1980. Evidence for 2 Fossil Spreading Ridges in the Southeast Pacific. GEol. Soc. Am. Bull. 91 (5), 263–271.

Marchig, V., Reyss, J.L., 1984. Diagenetic mobilization of manganese in Peru Basin sediments. Geochim. Cosmochim. Acta 48, 1349–1352.

Marchig, V., von Stackelberg, U., Wiedicke, M., Durn, G., Milovanovic, D., 1999. Hydrothermal activity associated with off-axis volcanism in the Peru Basin. Mar. Geol. 159, 179–203.

Marcon, Y., Sahling, H., MacDonald, I.R., Wintersteller, P., Ferreira, C.d.S., Bohrmann, G., 2018. SLOW VOLCANOES the intriguing similarities between marine Asphalt and Basalt Lavas. Oceanography 31, 194–205.
Meschede, M., Barckhausen, U., Worm, H.U., 1998. Extinct spreading on the Cocos Ridge. Terra Nova 10, 211–216.
Meschede, M., Barckhausen, U., Engels, M., Weinrebe, W., 2008. The trace of the Pacific-Cocos-Nazca triple junction in the Central Pacific and the formation of an overlapping spreading centre. Terra Nova 20, 246–251.
Morgan, W.J., 1971. Convection plumes in the lower mantle. Nature 230, 42–43.
Pälike, H., Lyle, M.W., Nishi, H., Raffi, I., Ridgwell, A., Gamage, K., Klaus, A., Acton, G., Anderson, L., Backman, J., Baldauf, J., Beltran, C., Bohaty, S.M., Bown, P., Busch, W., Channell, J.E.T., Chun, C.O.J., Delaney, M., Dewangan, P., Dunkley Jones, T., Edgar, K.M., Evans, H., Fitch, P., Foster, G.L., Gussone, N., Hasegawa, H., Hathorne, E.C., Hayashi, H., Herrle, J.O., Holbourn, A., Hovan, S., Hyeong, K., Iijima, K., Ito, T., Kamikuri, S.-i., Kimoto, K., Kuroda, J., Leon-Rodriguez, L., Malinverno, A., Moore, T.C.J., Murphy, B.H., Murphy, D.P., Nakamura, H., Ogane, K., Ohneiser, C., Richter, C., Robinson, R., Rohling, E.J., Romero, O., Sawada, K., Scher, H., Schneider, L., Sluijs, A., Takata, H., Tian, J., Tsujimoto, A., Wade, B.S., Westerhold, T., Wilkens, R., Williams, T., Wilson, P.A., Yamamoto, Y., Yamamoto, S., Yamazaki, T., Zeebe, R.E., 2012. A Cenozoic record of the equatorial Pacific carbonate compensation depth. Nature 488, 609–614.
Paul, S.A.L., Haeckel, M., Bau, M., Bajracharya, R., Koschinsky, A., 2019. Small-scale heterogeneity of trace metals including REY in deep-sea sediments and pore waters of the Peru Basin, SE equatorial Pacific. Biogeosciences 16, 4829–4849.
Rea, D.K., Leinen, M., 1985. Neogene history of the calcite compensation depth and lysocline in the South-Pacific Ocean. Nature 316, 805–807.
Sandwell, D., Fialko, Y., 2004. Warping and cracking of the Pacific plate by thermal contraction. J. Geophys. Res. 109, 12.
Sato, Y., Hirano, N., Machida, S., Yamamoto, J., Nakanishi, M., Ishii, T., Taki, A., Yasukawa, K., Kato, Y., 2018. Direct ascent to the surface of asthenospheric magma in a region of convex lithospheric flexure. Int. Geol. Rev. 60, 1231–1243.
Segl, M., Mangini, A., Bonani, G., Hofmann, H.J., Nessi, M., Suter, M., Wolfli, W., Friedrich, G., Pluger, W.L., Wiechowski, A., Beer, J., 1984. Be-10-dating of a manganese crust from central North Pacific and implications for ocean palaeocirculation. Nature 309, 540–543.
Simon-Lledo, E., Bett, B.J., Huvenne, V.A.I., Koeser, K., Schoening, T., Greinert, J., Jones, D.O.B., 2019. Biological effects 26 years after simulated deep-sea mining. Sci. Rep. 9, 13.
Smith, W.H.F., Sandwell, D.T., 1997. Global sea floor topography from satellite altimetry and ship depth soundings. Science 277, 1956–1962.
Steinberger, B., 2000. Plumes in a convecting mantle: Models and observations for individual hotspots. J. Geophys. Res. Solid Earth 105, 11127–11152.
Thiel, H., Schriever, G., Ahnert, A., Bluhm, H., Borowski, C., Vopel, K., 2001. The large-scale environmental impact experiment DISCOL – reflection and foresight. Deep-Sea Res. II Top. Stud. Oceanogr. 48, 3869–3882.
Toomey, D.R., Wilcock, W.S.D., Solomon, S.C., Hammond, W.C., Orcutt, J.A., 1998. Mantle seismic structure beneath the MELT region of the East Pacific Rise from P and S wave tomography. Science 1224–1227.
van der Heijden, K., Petersen, J.M., Dubilier, N., Borowski, C., 2012. Genetic connectivity between North and South Mid-Atlantic ridge chemosynthetic bivalves and their symbionts. PLoS One 7.
Van Dover, C., Humphris, S., Fornari, D., Cavanaugh, C., Collier, R., Goffredi, S., Hashimoto, J., Lilley, M., Reysenbach, A., Shank, T., Von Damm, K., Banta, A., Gallant, R., Gotz, D., Green, D., Hall, J., Harmer, T., Hurtado, L., Johnson, P., McKiness, Z., Meredith, C., Olson, E., Pan, I., Turnipseed, M., Won, Y., Young, C., Vrijenhoek, R., 2001. Biogeography and ecological setting of Indian Ocean hydrothermal vents. Science 294, 818–823.
Wiedicke, M.H., Weber, M.E., 1996. Small-scale variability of seafloor features in the northern Peru basin: results from acoustic survey methods. Mar. Geophys. Res. 18, 507–526.
Yeo, I., Searle, R.C., Achenbach, K.L., Le Bas, T.P., Murton, B.J., 2012. Eruptive hummocks: building blocks of the upper ocean crust. Geology 40, 91–94.